Published in "Chemistry - A European Journal 19(5): 1754–1761, 2013"
which should be cited to refer to this work.

pH-Dependent Coordination of Ag^{I} Ions by Histidine: Experiment, Theory, and a Model for SilE

Laurent Mirolo,[a] Tobias Schmidt,[b] Sonja Eckhardt,[a] Markus Meuwly,[b] and Katharina M. Fromm*[a]

Abstract: Artificial implants and biomaterials lack the natural defense system of our body and, thus, have to be protected from bacterial adhesion and biofilm formation. In addition to the increasing number of implanted objects, the resistance of bacteria is also an important problem. Silver ions are well-known for their antimicrobial properties, yet not a lot is known about their mode of action. Silver is expected to interact on many levels, thus the development of silver resistance is very difficult. Nevertheless, some bacteria are able to resist silver, even at higher concentrations. One such defense mechanism of bacteria against heavy-metal intoxication includes an efflux system. SilE, a periplasmic silver-binding protein that is involved in this defense mechanism, has been shown to possess numerous histidine functions, which strongly bind to silver atoms, as demonstrated by ourselves previously. Herein, we address the question of how histidine binds to silver ions as a function of pH value. This property is important because the local proton concentration in cells varies. Thus, we solved the crystal structures of histidine–silver complexes at different pH values and also investigated the influence of the amino-acid configuration. These results were completed by DFT calculations on the binding strength and packing effects and led to the development of a model for the mode of action of SilE.

Keywords: bacteria · density functional calculations · histidine · silver · X-ray diffraction

Introduction

The number of patients that require joint replacement or internal-fixation devices is steadily increasing. For example, knee replacement has become a routine surgery; each year, it is performed on over 500,000 people in the US alone[1] and this value is increasing annually.[2] With an overall infection rate of, for example, about 5% for orthopedic implants,[3] bacterial contamination is one of the most important complications. These implant infections occur frequently, either perioperatively, by bacterial contamination of the surgical site, of which mostly low-virulence organisms, including *S. epidermidis,* are responsible, or postoperatively, by hematogenous infections.[4] These latter infections are the result of the seeding of the implant site by organisms that are transported there in the bloodstream from another infected region. Bacteria on implants typically proliferate and cluster in multilayers of exopolysaccharides, known as biofilms; this structure allows bacteria to resist antimicrobial agents and immune responses.[5] An attractive concept for infection prevention is the coating of the surface of implant materials with bactericidal compounds.[6] One example is a coordination-polymer network based on silver, which has been synthesized and studied as a nanostructure coating and an effective antimicrobial agent.[7] In the past, various mechanisms for the bactericidal activity of silver have been described and, with the increasing bacterial resistance against antibiotics, silver chemistry has felt a revival in a medical context. Silver ions are known to react with electron-donor groups that contain nitrogen, oxygen, or sulfur atoms that are present in bacteria as, for example, amino, imidazole, phosphate, carboxy, or thiol functional groups in enzymes, proteins, or in DNA.[8]

The widespread use of silver in medicinal chemistry, such as in burn wounds, where silver sulfadizine and silver-impregnated nylon cloths are used as antiseptics, has inevitably led to the isolation of "silver-resistant" bacteria.[9] However, the mechanisms that lead to silver resistance are still not well-understood. In the literature, there is still an ongoing discussion of whether there is a real resistance towards silver or whether the "resistant" bacteria are simply able to eliminate the silver species. Silver et al. reported plasmid pMG101, which was isolated from a silver-resistant strain of *Salmonella*. Up to now, the function of eight out of the nine genes that have been found to be responsible for the silver

[a] L. Mirolo,[+] Dr. S. Eckhardt,[+] Prof. Dr. K. M. Fromm
Department of Chemistry
Fribourg Center for Nanomaterials
University of Fribourg
Chemin du musée 9, 1700 Fribourg (Switzerland)
Fax: (+41) 26-300-97-38
E-mail: katharina.fromm@unifr.ch

[b] T. Schmidt,[+] Prof. Dr. M. Meuwly
Department of Chemistry, University of Basel
Klingelbergstrasse 80, 4056 Basel (Switzerland)

[+] These authors contributed equally to this work.

Supporting information for this article is available

resistance of this plasmid has been determined.[9] These genes encode for a chemiosmotic efflux pump, an ATPase efflux pump, and two periplasmic silver-binding proteins, SilE and SilF. SilE is a 143-amino-acid-long protein and, of these, 10 histidine residues are proposed as the primary candidates for metal binding.[10,11] The fact that this metal-binding protein is only synthesized during bacterial growth in the presence of Ag^I ions makes SilE an interesting target for the understanding of silver resistance.

Recently, we demonstrated that certain amino-acid sequences within libraries of tri- and tetrapeptides showed preferential binding of silver ions and their subsequent reduction into silver nanoparticles, whereas other sequences did not bind silver ions at all.[12] A brief excursion into the scientific literature revealed that, in recent years, different computational methods have been applied for the calculation of the silver affinity of all twenty naturally occurring amino acids;[13–15] however, to the best of our knowledge, there has only been one comparable experimental study that was based on mass spectrometry.[16] Both computational and experimental data rate histidine as one of the preferential binding sites for silver ions. Depending on the nature of the amino acid, such binding can only occur through the two termini or through the side-chain. For histidine, this side-chain participation has been calculated to be stronger than the contribution of the termini.[13] However, solid-state structures and, hence, details of the binding situation of silver ions by amino acids are still scarce.[17] Regardless of the lack of structural information, the coordination of amino acids, peptides, or even proteins to silver ions has found application as analytical tool, for example, in mass spectrometry[18] or for the determination of cysteine levels.[19]

To contribute to the wider understanding of the binding mechanisms, we set out to investigate the binding modes of histidine towards silver ions; thus, herein, we report on the pH-dependent coordination of histidine towards silver ions. These results are completed by theoretical studies on the binding strength and packing effects in the three compounds studied herein.

Results and Discussion

With the aim of studying silver–histidine complexes at different pH values, we attempted to crystallize the reaction mixture of $AgNO_3$ and histidine at basic pH values, disappointingly without success. Literature reports have described an elegant route to silver–histidine complexes by reacting Ag_2O with histidine (His).[17d,h]

One compound has been proposed to be a water-soluble molecular complex of Ag/His (1:1), with EtOH present in the solid state, but its structure is hitherto unknown.[17d] Starting from histidine and $AgNO_3$, Nomiya and co-workers did not report any interpretable result. However, from the reaction between Ag_2O and histidine, a coordination polymer was obtained upon standing and slow crystallization for which the structure could be solved, thus revealing a left-handed helical coordination polymer (**A**) for L-His[17d] and its right-handed mirror image (**B**) for D-His[17h] (Figure 1). In both cases, the histidine ligands connected the silver ions together by binding through the imidazole nitrogen atom on one hand, and the N atom of the NH_2 group on the other. Disappointingly, the positions of the protons are not clear from the X-ray structures, but the coordination mode of histidine towards the silver ions indicates that the amino acid is present it its zwitterionic state. The exact pH conditions during these reactions were also not described within that publication.

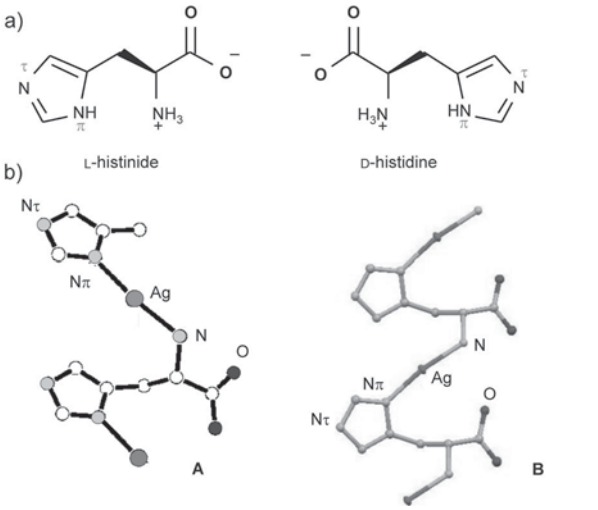

Figure 1. a) Structures of L- and D-histidine at neutral pH value; b) 1D chains that are formed by the interactions between silver ions and L- (**A**) and D-histidine (**B**). Modified/reproduced with permission from Nomiya et al.,[17d] Copyright (2000) American Chemical Society, and Kasuga et al.,[17h] Copyright (2011) Elsevier Limited.

Given the amount of effort that has been invested in obtaining solid-state structures of amino-acid complexes, and with silver ions in particular, it is even more surprising that we were able to obtain single crystals from a mixture of histidine and $AgNO_3$ under different pH conditions.

L-Histidine at neutral pH: **[{Ag(L-histidine)$_2$NO$_3$}$_2$]H$_2$O (1)**: Compound **1** is obtained from the reaction of silver nitrate with L-histidine at neutral pH. It crystallizes as colorless needles in the orthorhombic, chiral space group $P2_12_12$ (no. 18, see the Supporting Information, Table S1). The asymmetric unit is composed of one silver ion, two L-histidine ligands, one nitrate ion (Figure 2), and half a water molecule. A discrete complex is formed, in which the silver ion is almost linearly coordinated by two histidine molecules through nitrogen atoms N2 and N5 of the imidazole groups to form the moiety "His–Ag–His". The Ag–N distances are 2.109(3) and 2.098(3) Å and the N–Ag–N angle is 176.16(12)°. The two coordinating imidazole rings are approximately coplanar, with an angle of 15.78(13)° between the mean ring planes, whereas both α-amino-acid moieties of the two histidine molecules are pointing in the same direction (Figure 2). The H atoms can be localized in a Fouri-

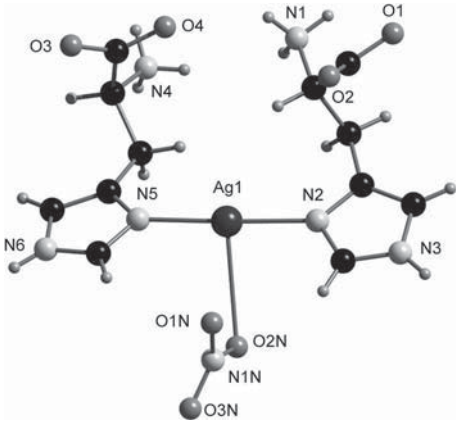

Figure 2. Asymmetric unit in complex **1**; the water molecule is omitted for clarity. O1N, O2N, and N1N stand for the nitrate-bound atoms.

er map, which shows that both His ligands are present as zwitterions, in which the NH_2 groups are protonated whilst the acid functions are deprotonated. The preference of silver ions for the softer N atoms of the imidazole rings versus the negatively charged C terminus is clearly demonstrated. Indeed, the coordination of the negatively charged carboxylate group would bring the metal cation closer to the protonated amine function, which would be unfavorable, owing to charge repulsion.

Besides the coordination of the amino-acid ligands, a nitrate anion binds to the silver cation through atom O2N, with a distance of 2.871(2) Å, thus indicating a weak bonding interaction. Additional π interactions between the two imidazole rings of the histidine molecules are present above and below the silver ion, owing to the arrangement of the complexes relative to each other (Figure 3), which demonstrates the soft character of the metal ion. Indeed, these distances are approximately 3.1 and 3.2 Å from the metal ion to the mean ring planes of the imidazole moieties.

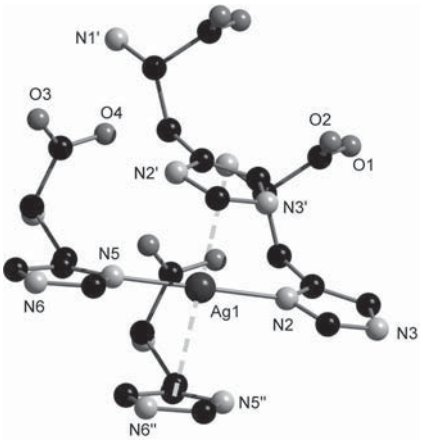

Figure 3. Intermolecular π interactions in compound **1** between the imidazole rings and the silver atom, as indicated by the dashed lines; hydrogen atoms have been omitted and the two histidine moieties that are responsible for the π interactions have been truncated for clarity. Symmetry codes: (′) *x*, *y*, *z*−1; (″) *x*, *y*, *z*+1. Distances: Ag–plane *z*−1: 3.181 Å; Ag–plane *z*+1: 3.124 Å.

In the packing of compound **1**, the nitrate anion connects one complex to two others through H bonds with the protonated N atoms of neighboring imidazole moieties. Thus, (nitrate oxygen) atoms O1N and O3N bind to the N6 atom of one molecule, whilst the O2N and O3N atoms are connected to the N3 atom of another neighboring complex (see the Supporting Information, Figure S1). Thus, two layers of $[Ag(His)_2]$ moieties are connected in a head-to-head fashion through nitrate anions, by considering the imidazole rings as "head" parts of the molecules. On the other hand, the tails of the complexes are also linked to each other through H-bonding interactions between the ammonium and carboxylate groups and through H-bonding interactions between the carboxylate groups, which are mediated by water molecules. The so-formed layer structure is shown in the Supporting Information, Figure S2, and the detailed H-bonding network is described in the Supporting Information, Table S2.

The coordination mode of histidine towards silver ions in compound **1** is probably the same as that in biological media because the pK_a value of the imidazole side-chain is 6.0, thus leading to an isoelectric point of 7.6, which is close to the physiological pH value.[20] However, the local presence of protons might lead to temporary protonation of the amino-acid side-chain. Indeed, pH-triggering could be one mechanism for controlling the binding and release of silver ions, as required by heavy-metal ion pumps or metal-binding peptides. In such cases, the protonation of certain binding sites that are available at neutral pH could become preferentially blocked by protons, thereby leading to a release of the bound metal ions. Therefore, we also addressed the question of whether silver-ion coordination by histidine was possible at low pH values and, if so, how the coordination mode and binding energies changed.

L-Histidine at acidic pH values: **$[(\{Ag(L\text{-histidinium})(NO_3)_2\}_2)H_2O]_n$ (2)**: Compound **2** is obtained from the reaction between $AgNO_3$ and L-histidine under acidic conditions (HNO_3) and crystallizes as colorless needles in the triclinic space group *P*1 (no. 1, see the Supporting Information, Table S1). The principal building unit of this coordination polymer is comprised of two silver atoms, two protonated L-histidinium moieties, four nitrate anions, and a water molecule (Figure 4). Within this asymmetric unit, two silver ions, Ag1 and Ag2, are bridged by the two oxygen atoms (O1 and O2) of the carboxylate moiety of one histidine ligand and by one oxygen atom (O3) of a carboxylate unit of a second histidine ligand (Ag1−O1 2.226(4) Å, Ag1−O3 2.216(4) Å, Ag2−O2 2.243(4) Å, Ag2−O3 2.716(5) Å). The second oxygen atom of this latter unit (O4) coordinates to a silver ion (Ag2′) in the next asymmetric unit (Ag2′−O4 2.299(4) Å); thus, this atom (Ag2′) is less than 3 Å away from atom Ag1 (Σ(van der Waals Ag radii) 3.44 Å),[21] such that a Ag−Ag interaction can be considered.[22] The Ag2 and Ag2′ ions are pairwise bridged by the O4N and O6N atoms of one nitrate anion (Ag1−O1N 2.392(7) Å, Ag2−O4N 2.510(7) Å). On the other hand, atom Ag1 carries another nitrate anion, with binding only through atom O1N.

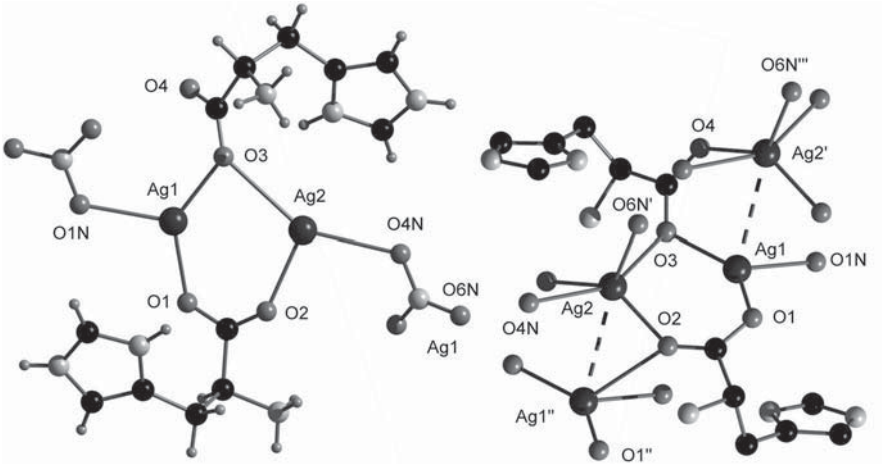

Figure 4. Left: Direct coordination within the asymmetric unit of complex **2**; the two non-coordinating nitrate molecules and a water molecule have been omitted for clarity. Right: Asymmetric unit in compound **2** and its closest neighbors; hydrogen atoms have been omitted for clarity. Symmetry codes: (′) $x-1, y, z$; (″) $x+1, y, z$; (‴) $x-2, y, z$.

Hence, each unit cell contains an L-histidinium moiety and its mirror image, a D-histidinium moiety, as ligands. The carboxylate groups of both histidine enantiomers face each other and act as bidentate O-donor ligands in linking two silver ions, Ag1 and Ag1′, together (Figure 5). The so-connected silver atoms have, with a distance of 2.814(1) Å, a short contact to each other, which is indicative of strong interactions between them.[21,22]

Whereas the O2 atom of the carboxylic group of each histidine ligand only binds to silver atom Ag1′ (2.250(1) Å), the O1 atom of the same group is connected to silver atom Ag1 of the dimer, through a short distance of 2.300(1) Å, and to atom Ag1′ of the next dimer unit, with a longer distance of 2.456(1) Å (see the Supporting Information, Figure S5). Each such pair of silver atoms is further connected to the next pair through nitrate ions. That is, one nitrate ion acts as a bidentate ligand, connecting every second silver ion. There are two nitrate anions, one of which bridges from atom Ag1 to its translational equivalent, whilst the second connects atom Ag1′ to its translational equivalent. Thus, each of the silver ions is coordinated by two oxygen atoms from two different carboxylate groups within the pair of Ag ions, one oxygen atom of a carboxylic group of the neighbor unit, and one O-atom of a nitrate ion. As for compound **2**, it is surprising how the anions concentrate around the positive charge of the silver ions, rather than the ammonium group or the protonated imidazole rings. However, H-bonding interactions occur between the

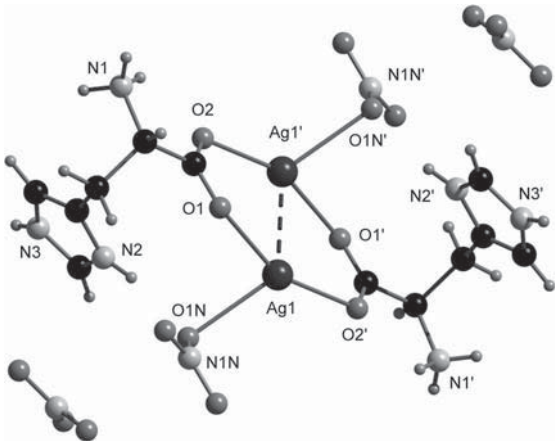

Figure 5. Two asymmetric units in complex **3**. Symmetry code: (′) $-x, -y, 2-z$.

This nitrate anion is involved in H-bonding interactions to the protonated imidazole rings of a histidine ligand in the same 1D chain (see the Supporting Information, Figure S3), to the protonated ammonium function of a histidine ligand in a parallel strand, and to the intercalated water molecule (O1W). This water molecule forms further H bonds to the free oxygen atom of the nitrate anion that bridges the Ag2 ions (O5N) and acts as H-bond acceptor from protonated NH_2 groups of parallel chains. Two further nitrate anions are not connected to silver ions, but are intercalated between the imidazolium moieties of neighboring chains, thereby forming H bonds to the protonated N atoms (see the Supporting Information, Figure S4 and Table S3).

It is amazing to see that, in compound **2**, each silver ion, in addition to being coordinated by a negatively charged carboxylate moiety of the histidinium group ($pK_a1 = 1.82$),[20] is connected to at least one nitrate anion, whilst the positively charged histidine parts are involved in H-bonding interactions. In compound **1**, the silver ion clearly prefers the neutral parts of the ligand, whilst the nitrate ion is 0.4–0.7 Å further away than in compound **2**. This difference led to further investigation of these compounds by using theoretical methods (see the Computational Studies section).

In parallel to the pure L-histidine compounds, we also investigated the coordination behavior of a racemic mixture of D- and L-histidine towards silver ions.

DL-Histidine at acidic pH values: **$[Ag_2$(L-histidinium)(D-histidinium)$(NO_3)_4]_n$ (3)**: Compound **3** crystallizes under similar conditions as compound **2** in the form of colorless needles in the triclinic space group *P*1 (no. 2, see the Supporting Information, Table S1). There are two asymmetric units per unit cell, each of which is comprised of one silver atom, one histidinium ion, and two nitrate anions. Notably, because a racemic mixture of histidine was used for crystallization, it allowed the structure to be centrosymmetric.

non-coordinating O atoms of the nitrate group and the ammonium moiety, as well as with the protonated imidazole rings, thereby connecting the moieties into a 3D network (see the Supporting Information, Figure S6 and Table S4).

In summary, the coordination mode of histidine towards silver is strongly influenced by the pH value of the medium, thereby changing from side-chain coordination under neutral conditions to coordination through the negatively charged C terminus under more-acidic conditions, where the imidazole side-chain is protonated. This change is accompanied by an altering of the histidine/silver ratio from 2:1 under neutral conditions (**1**) to 1:1 under acidic conditions (**2** and **3**). In contrast, the configuration of the amino acid seems to be less important, because structures **2** and **3** are quite similar: Both coordinate to silver ions through the histidine C terminus at acidic pH values. This result is in agreement with the results of Nomiya and co-workers,[17d,h] who showed that the configuration of the amino acid influenced the helicity of the obtained helices upon coordination of silver but not the coordination mode itself (Figure 1).

Computational studies: Given the different possible coordination modes of histidine towards silver ions, depending on the pH value, we wanted to obtain a better understanding of the binding situation in each of the described compounds (**1**–**3**). Thus, we investigated the environment of each silver atom for structural fragments of compounds **1**–**3** (see the Supporting Information, Table S5) and calculated the energy that was required to remove the metal ion from its binding site. The results are shown in Table 1, relative to the stabilization energy of complex **1**. The silver–ligand interactions are most favorable for this complex because the energy that is necessary to remove the silver ion from the complex is significantly larger than for the other complexes. For complexes **2** and **3**, the stabilization energies lie in the same range and the histidine ligands are in a doubly protonated—and, thus, positively charged—state. This result leads to a high overall charge in the fragments of complexes **2** and **3**, whereas complex **1** is neutral. To investigate the influence of this overall charge on the calculations, we designed a neutral system (see the Experimental Section), in which the histidine groups were singly protonated at the π position (for nomenclature, see Figure 1) and, thus, were neutral. Also, for the neutral system, the results (Table 1) suggest that complex **1** has the most-favorable silver–ligand interactions but the relative stabilization energies for complex **2** and **3**, in comparison to compound **1**, are significantly smaller than in the charged system.

Table 1. Calculated relative binding energies [kcal mol^{-1}] of the silver ions in complexes **1**–**3**.[a]

Complex	Ag1	Ag2
$[\{Ag(\text{L-histidine})_2NO_3\}_2]H_2O$ (**1**)	0.0	–
$[(\{Ag(\text{L-histidinium})(NO_3)_2\}_2)H_2O]_n$ (**2**)	286.6/15.1	272.2/1.7
$[Ag_2(\text{L-histidinium})(\text{D-histidinium})(NO_3)_4]_n$ (**3**)	281.6/6.1	281.6/6.1

[a] For compound **1**, only one silver ion is present, whereas, for compounds **2** and **3**, two different silver ions are present. For complexes **2** and **3**, two relative binding energies are shown, which represent the values for the charged and neutral systems, respectively.

One reason for the less-favorable stabilization of complexes **2** and **3** compared to complex **1** is the close proximity between the two Ag^I ions in complexes **2** and **3**. To characterize the amount of unfavorable interaction energy that is due to this close proximity, the energy that was required to form a Ag_2^{2+} system with the same Ag–Ag distance as that observed in the crystal structures was calculated. This unfavorable interaction contributes 103.6 kcal mol^{-1} to the destabilization of complexes **2** and **3**. To compare this interaction energy in a vacuum with that in the complex, the interaction energy of the Ag_2^{2+} system within the complex was computed. A slight decrease in the unfavorable interaction energy was observed in the complex, with calculated interaction energies of 96.8 and 99.5 kcal mol^{-1} for complexes **2** and **3**, which corresponds to a decrease in the unfavorable energy of the Ag–Ag interaction by 6.8 and 4.1 kcal mol^{-1}, respectively. Surprisingly, the neutral compound (**1**), which shows the softest coordination of the silver ion, with a coordination of four imidazole rings and one distant nitrate group, seems to be the strongest for this metal ion. The stability of this specific site is certainly improved by the side-on coordination of the neighboring imidazole rings, which contribute through metal–π interactions (Figure 3).

In the other cases (**2** and **3**), the nitrate anions and carboxylate groups act as negatively charged ligands and help to stabilize the cation and diminish the partial charge on the silver ions. The calculated partial charges for the three complexes are shown in Figure 6.

In complexes **2** and **3**, a slight increase in the partial charge on the silver ions is observed compared to complex **1**. This increase is also the case for the silver-ion environment in compounds **2** and **3**, which is more negatively charged than that in compound **1**. The more-polar environment around the silver ion enhances the stability of the Ag_2^{2+} system in these structures (**2** and **3**), and explains the slight decrease in the unfavorable interaction energy observed in the complexes compared to the vacuum. (Table 1).

For further insight into the binding situation around the silver ions in complexes **1** to **3**, the conformational-strain energy of the histidine residues in each crystal structure was calculated (Table 2). Interestingly, for structures **2** and **3**, the two histidine residues show similar internal strains, whereas, for structure **1**, the calculated values for the two histidine residues are different. This inequality is caused by different

Table 2. Calculated conformational strain [kcal mol^{-1}] of the two histidine residues in the complex for each crystal structure.

Complex	His1	His2
$[\{Ag(\text{L-histidine})_2NO_3\}_2]H_2O$ (**1**)	36.9	45.3
$[(\{Ag(\text{L-histidinium})(NO_3)_2\}_2)H_2O]_n$ (**2**)	37.6	37.0
$[Ag_2(\text{L-histidinium})(\text{D-histidinium})(NO_3)_4]_n$ (**3**)	35.5	35.5

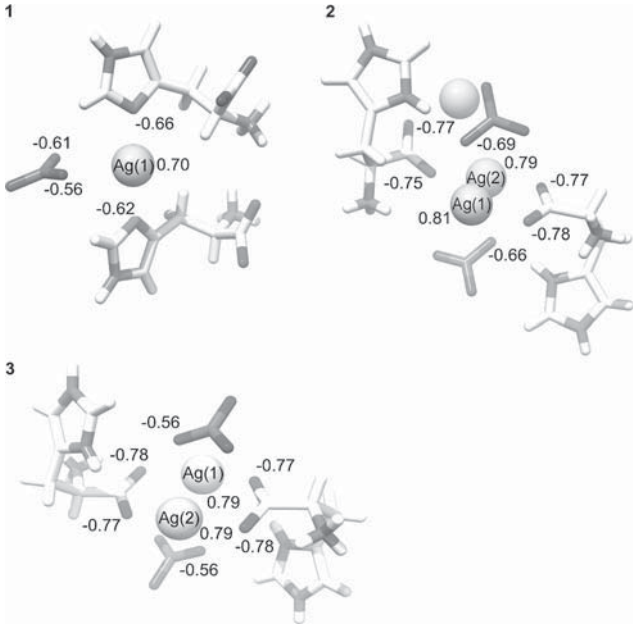

Figure 6. Calculated partial charges by using NBO analysis on fragments of crystals **1**–**3**. Silver ions are labeled according to the naming used in the calculations.

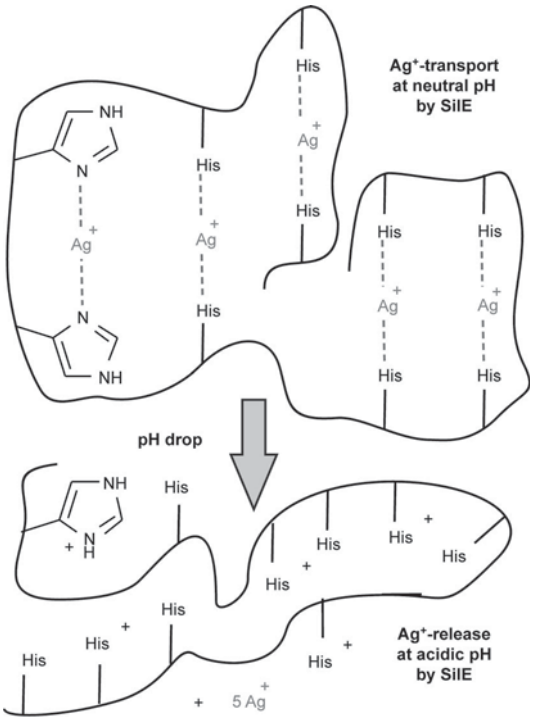

Scheme 1. Proposed mode of action of SilE in the transport of silver ions in bacterial cells: The silver ions are strongly bound at neutral pH, as shown for compound **1**, but they are released close to an efflux pump at acidic pH values, thereby resulting in the loss of the secondary structure of SilE.

orientations in both the ammonium groups and the imidazole planes of the histidine groups.

With both experimental and theoretical data in hand, we propose a mechanism for the function of the periplasmic silver-binding protein, SilE. Because the outer membrane acts as a Donnan membrane, the pH value of the periplasmic space is known to depend on the pH value of the surrounding medium.[23] Thus, at physiological pH, silver ions can be bound by the neutral imidazole side-chains in a silver/histidine ratio of 2:1, similar to compound **1** (Scheme 1), thus confirming the hypothesis of Silver et al.[9] At neutral pH, the calculations show that the silver ions are well-bound, so that a directed transport to the chemiosmotic efflux pump can occur without the loss of silver. All other coordination modes of the carboxylate groups are shown to be weaker and, therefore, will not contribute significantly to the scavenging of silver ions within the cell. Upon local changes in the pH value to below 6, which correspond to the pK_a of the histidine side-chain, the imidazole ring becomes protonated, thereby resulting in a loss of binding energy, as shown for compounds **2** and **3**, and, hence, to the release of silver. From the related Cus system, it is known that the metal-binding protein CusF interacts with the proteins on the chemiosmotic efflux pump (CusCBA),[24] thus bringing the metal-binding protein into the proximity of the proton gradient from the outside to the inside of the cell. This movement would, in the case of SilE, lead to protonation of the imidazole side-chains that are near to the efflux pump (SilCBA) and, thus, the release of silver cations into the periplasmic space, from where they have to be transported to the outside of the cell. According to the switching mechanism, which is one of the two mechanisms that are currently under discussion in the literature for the related Cus–efflux complex,[25] this periplasmic efflux takes place when the metal-ion concentration close to the efflux pump is high enough, thereby leading to a conformational change in one of the subunits of the efflux pump (CusB) that allows the metal ions to enter the pump. Because the exact mechanism of this metal-ion detoxification is still controversial, our results might provide further insight into the complex process of metal-ion extrusion.

Conclusion

In conclusion, we have found that the bonding of silver ions by histidine ligands is stronger under neutral conditions than under acidic conditions. This result corresponds well with the neutral pH conditions in the human body. Thus, the silver-binding moiety of the ligand is solely the imidazole ring on the amino-acid side-chain. Yet, in the presence of acid, the silver atom is displaced from its coordination site, owing to protonation of the imidazole rings; this displacement is the case in both stereochemically pure and racemic mixtures of the amino acid. This dislocation might be responsible for the efflux-pump mechanism that is found in bacteria, which have been discussed as being resistant to silver. The bonding behavior of histidine towards silver ions

confirms our earlier observations when we studied the selectivity for silver binding of tri- and tetrapeptides.[12] Our studies have shown that the binding sites, binding geometry, and charge on the binding site may vary dramatically under the influence of pH value.

Experimental Section

General information: The starting materials were commercially available and were used without further purification. Doubly distilled water was used as the solvent. ^{1}H NMR spectra were recorded on a Bruker Advance DPX 360 MHz spectrometer and the residual solvent signal was used for calibration (D_2O, $\delta = 4.79$ ppm).[26] MS was performed on a Bruker Esquire HTC mass spectrometer. FTIR measurements were performed on a Bruker FTIR Tensor 27 spectrophotometer.

Synthesis: **[{Ag(L-histidine)$_2$NO$_3$}$_2$]H$_2$O (1)**: Silver nitrate (170 mg, 1 mmol) and L-histidine (155 mg, 1 mmol) were added into a test tube into which water (10 mL) was poured. After sonication, the clear solution was stored in the dark for 3 days. Slow evaporation of the water allowed crystals to grow after several days (214 mg, 0.2 mmol, 44% yield). The uniformity of the product was confirmed by powder X-ray diffraction. ^{1}H NMR (360 MHz, D_2O, 300 K): $\delta = 7.95$ (s, 1H; Im-H), 7.18 (s, 1H; Im-H), 4.16 (t, ^3J(H,H) = 6.1 Hz, 1H; α-H), 3.26 ppm (d, ^3J(H,H) = 6.1 Hz, 2H; β-H); FTIR (solid): $\tilde{\nu} = 3119$ (NH_3^+), 3018 (C=C-H), 2990 (C–H), 1620, 1589, 1564, 1504 (NH_3^+, COO^-, C=C), 1383, 1312, 1285 cm^{-1} (C–O); MS (70 eV): m/z (%): 419 (91) $[C_{12}H_{18}AgN_6O_4]^+$, 417 (100) $[C_{12}H_{18}AgN_6O_4]^+$, 262 (20) $[C_6H_9AgN_3O_2]^+$, 264 (19) $[C_6H_9AgN_3O_2]^+$.

[({Ag(L-histidinium)(NO$_3$)$_2$}$_2$)H$_2$O]$_n$ (2): Silver nitrate (170 mg, 1 mmol) and L-histidine (155 mg, 1 mmol) were added into a test tube into which water (10 mL) was poured. Nitric acid (65%) was added until a pH value of 3–4 was reached to obtain the protonated form of histidine. The clear solution was stored in the dark for 3 days. Slow evaporation of the water allowed crystals to grow after several days (365 mg, 0.46 mmol, 92% yield). The uniformity of the product was confirmed by powder X-ray diffraction. ^{1}H NMR (360 MHz, D_2O, 300 K): $\delta = 8.63$ (s, 1H; Im-H), 7.37 (s, 1H; Im-H), 4.16 (t, ^3J(H,H) = 6.6 Hz, 1H; α-H), 3.39 (dd, ^2J(H,H) = 16.1 Hz; ^3J(H,H) = 6.6 Hz, 1H; β-H), 3.33 ppm (dd, ^2J(H,H) = 16.1 Hz, ^3J-(H,H) = 6.1 Hz, 1H; β-H); FTIR (solid): $\tilde{\nu} = 3105$ (NH_3^+), 3008 (C=C–H), 2925 (C–H), 1620, 1572, 1502 (NH_3^+, COO^-, C=C), 1334, 1287 cm^{-1} (C–O)); m/z (%): 419 (81) $[C_{12}H_{18}AgN_6O_4]^+$, 417 (100) $[C_{12}H_{18}AgN_6O_4]^+$, 262 (38) $[C_6H_9AgN_3O_2]^+$, 264 (33) $[C_6H_9AgN_3O_2]^+$.

[Ag$_2$(L-histidinium)(D-histidinium)(NO$_3$)$_4$]$_n$ (3): Silver nitrate (170 mg, 1 mmol) and D/L-histidine (155 mg, 1 mmol) were added into a test tube into which water (10 mL) was poured. Nitric acid (65%) was added until a pH value of 3–4 was reached to obtain the protonated form of histidine. The clear solution was stored in the dark for 3 days. Slow evaporation of the water allowed crystals to grow after several days (230 mg, 0.6 mmol 60% yield). The uniformity of the product was confirmed by powder X-ray diffraction. ^{1}H NMR (360 MHz, D_2O, 300 K): $\delta = 8.29$ (s, 1H; Im-H), 7.29 (s, 1H; Im-H), 4.04 (t, ^3J(H,H) = 6.3 Hz, 1H; α-H), 3.32 ppm (d, ^3J(H,H) = 6.3 Hz, 2H; β-H); FTIR (solid): $\tilde{\nu} = 3129$ (NH_3^+), 3020 (C=C–H), 2867 (C–H), 1621, 1584, 1498 (NH_3^+, COO^-, C=C), 1380, 1331, 1284 cm^{-1} (C–O)); m/z (%):419 (72) $[C_{12}H_{18}AgN_6O_4]^+$, 417 (100) $[C_{12}H_{18}AgN_6O_4]^+$, 262 (52) $[C_6H_9AgN_3O_2]^+$, 264 (44) $[C_6H_9AgN_3O_2]^+$.

Crystallographic data:[27] The crystallographic data were collected at 150 K on a Stoe IPDS 2T-Image Plate Diffraction System that was equipped with an Oxford Cryosystem open-flow cryostat[28] by using Mo Kα graphite-monochromated radiation. The structure was solved by using direct methods with the program SIR-2004.[29] Refinement and all further calculations were performed by using SHELXL-97.[30] The non-H atoms were refined anisotropically by using weighted full-matrix least-squares on F^2. The hydrogen atoms were included at calculated positions and treated as riding atoms by using the default parameters in SHELXL. The Diamond program was used for graphical representation of the structures.[31]

Crystal data for 1: $C_{24}H_{38}Ag_2N_{14}O_{15}$; $M_w = 978.42$ g mol^{-1}; orthorhombic; $P2_12_12$ (no. 18); $a = 33.66280(10)$, $b = 9.7125(3)$, $c = 5.2157(8)$ Å; $V = 1705.3(3)$ Å^3; $Z = 4$; $\rho_{calcd} = 1.906$ mg m^{-3}; $F(000) = 988$; $T = 150(2)$ K; $\lambda = 0.71073$ Å; μ(Mo Kα) = 1.241 mm^{-1}; $2.18 < \theta < 19.98°$; 6610 reflections measured; 1563 unique reflections; 255 parameters refined; GOF (on F^2) = 1.072; $R1 = \Sigma|Fo-Fc|/\Sigma Fo = 0.0153$ and $wR2 = 0.0346$ for $I > 2\sigma(I)$; Flack parameter: −0.03(2).

Crystal data for 2: $C_{12}H_{22}Ag_2N_{10}O_{17}$; $M_w = 794.14$ g mol^{-1}; triclinic; $P1$ (no. 1); $a = 5.09440(10)$, $b = 9.1670(3)$, $c = 13.1855(4)$ Å; $a = 77.470(2)$, $b = 82.912(2)$, $\gamma = 79.988(2)°$; $V = 589.59(3)$ Å^3; $Z = 1$; $\rho_{calcd} = 2.237$ mg m^{-3}; $F(000) = 394$; $T = 293(2)$ K; $\lambda = 0.71073$ Å; μ(Mo Kα) = 1.767 mm^{-1}; $2.30 < \theta < 27.50°$; 17644 reflections measured; 5172 unique reflections; 372 parameters refined; 3 restraints; GOF (on F^2) = 1.064; $R1 = \Sigma|Fo-Fc|/\Sigma Fo = 0.0477$ and $wR2 = 0.1133$ for $I > 2\sigma(I)$; Flack parameter: −0.05(3).

Crystal data for 3: $C_6H_{10}AgN_5O_8$; $M_w = 388.06$ g mol^{-1}; triclinic; $P1$ (no. 2); $a = 5.1720(2)$, $b = 8.3581(3)$, $c = 13.5530(5)$ Å; $a = 94.146(3)$, $b = 95.462(3)$, $\gamma = 93.181(3)°$; $V = 580.54(4)$ Å^3; $Z = 2$; $\rho_{calcd} = 2.220$ mg m^{-3}; $F(000) = 384$; $T = 293(2)$ K; $\lambda = 0.71073$ Å; μ(Mo Kα) = 1.789 mm^{-1}; $2.98 < \theta < 23.99°$; 10061 reflections measured; 1809 unique reflections; 182 parameters refined; GOF (on F^2) = 1.182; $R1 = \Sigma|Fo-Fc|/\Sigma Fo = 0.0153$ and $wR2 = 0.0342$ for $I > 2\sigma(I)$.

Calculations: All calculations were performed with Gaussian 03, Revision D.02[32] at the DFT level by using the Becke three-parameter hybrid exchange functional and the Lee, Yang, and Parr correlation functional (B3LYP).[33] A split basis set with an effective core potential (LANL2DZ)[34] was used for all silver ions and the all-electron basis set 6–31G(d,p)[35] was employed for all other elements.

Complex stabilization of the silver ions: For each crystal structure, a fragment that consisted of multiple silver–ligand complexes was extracted for calculations, as described in the Supporting Information, Table S5. The energy that was required to remove a silver ion from its binding site in the complex was calculated according to the Equation (1), where complex–Ag$_{n-1}$ represents the full complex with one silver ion removed.

$$\text{complex}-\text{Ag}_{n-1} + \text{Ag}^{\text{I}} \rightarrow \text{complex}-\text{Ag}_n \quad (1)$$

The energy was computed as the difference between the single-point energies of the product and the reactants, according to Equation (2).

$$E(\text{complex}-\text{Ag}_n) - E(\text{complex}-\text{Ag}_{n-1}) - E(\text{Ag}^{\text{I}}) \quad (2)$$

For complexes **2** and **3**, two non-equivalent silver ions were present; for these above calculations, either one or the other was removed, as indicated by Ag1 or Ag2 in Table 1 and Figure 6.

Partial charges: For each structure, the partial charges on all atoms were calculated by performing a natural bond orbital (NBO) analysis.[36]

Energy of Ag–Ag interactions: The energies of the Ag1–Ag2 interactions were calculated as the difference between the single-point energies (in a vacuum) of $2Ag^I$ and Ag_2^{2+}, where the Ag–Ag distance was set to the distance that was observed in the crystal structure. To compare this interaction energy in a vacuum with the one in the complex, single-point energy calculations were performed in the complex and the interaction energy was computed according to Equation (3).

$$2\text{Ag}^{\text{I}} + \text{complex(2Ag removed)} \rightarrow \text{complex(whole)} \quad (3)$$

Conformational strain: The conformational strain of the histidine residues in the complexes was calculated for each crystal structure. Each histidine residue was extracted from the complex and, starting from this structure, two different optimizations were performed: Firstly, only the hydrogen atoms (all bonds to hydrogen atoms) were optimized to obtain conformations that were comparable between the three structures. Secondly, a full energy minimization was performed to obtain the fully relaxed conformations. Then, the internal strain energy was computed as the difference between the energies of the two corresponding structures

that were obtained from the optimization step.

Acknowledgements

The authors gratefully acknowledge financial support from the Swiss National Science Foundation (grant no. 200021–117810 to M.M.), the ProDoc Program, the Fribourg Center for Nanomaterials FriMat, and the NCCRnano.

[1] American Academy of Orthopaedic Surgeons (2010, March 14). A sporting chance for active total knee replacement patients. *ScienceDaily*. Retrieved September 16, 2011, from http://www.sciencedaily.com/releases/2010/03/100312071800.htm.

[2] T. Dixon, M. Shaw, S. Ebrahim, P. Dieppe, *Ann. Rheum. Dis.* **2004**, *63*, 825–830.

[3] C. von Eiff, G. Peters, C. Heilmann, *Lancet Infect. Dis.* **2002**, *2*, 677–685.

[4] T. W. Bauer, J. Parvizi, N. Kobayashi, V. Krebs, *J. Bone Joint Surg.* **2006**, *88A*, 869–882.

[5] F. Götz, *Mol. Microbiol.* **2002**, *43*, 1367–1378.

[6] P. S. Brunetto, K. M. Fromm, *Chimia* **2008**, *62*, 249–252.

[7] a) P. S. Brunetto, T. V. Slenters, K. M. Fromm, *Materials* **2011**, *4*, 355–367; b) T. V. Slenters, J. L. Sagué, P. S. Brunetto, S. Zuber, A. Fleury, L. Mirolo, A. Y. Robin, M. Meuwly, O. Gordon, R. Landmann, A. U. Daniels, K. M. Fromm, *Materials* **2010**, *3*, 3407–3429; c) O. Gordon, T. V. Slenters, P. S. Brunetto, A. E. Villaruz, D. E. Sturdevant, M. Otto, R. Landmann, K. M. Fromm, *Antimicrob. Agents Chemother.* **2010**, *54*, 4208–4218; d) T. V. Slenters, I. Hauser-Gerspach, A. U. Daniels, K. M. Fromm, *J. Mater. Chem.* **2008**, *18*, 5359–5362; A. Y. Robin, M. Meuwly, K. M. Fromm, H. Goesmann, G. Bernardinelli, *CrystEngComm* **2004**, *6*, 336–343.

[8] a) A. D. Russell, W. B. Hugo, *Prog. Med. Chem.* **1994**, *31*, 351–370; b) J. L. Clement, P. S. Jarrett, *Met. Based Drugs* **1994**, *1*, 467–482.

[9] S. Silver, L. T. Phung, G. Silver, *J. Ind. Microbiol. Biotechnol.* **2006**, *33*, 627–634.

[10] A. Gupta, K. Matsui, J.-F. Lo, S. Silver, *Nat. Med.* **1999**, *5*, 183–188.

[11] S. Silver, A. Gupta, K. Matsui, J.-F. Lo, *Met. Based Drugs* **1999**, *6*, 315–320.

[12] K. Belser, T. V. Slenters, C. Pfumbidzai, G. Upert, L. Mirolo, K. M. Fromm, H. Wennemers, *Angew. Chem.* **2009**, *121*, 3715–3718; *Angew. Chem. Int. Ed.* **2009**, *48*, 3661–3664.

[13] T. Shoeib, K. W. M. Siu, A. C. Hopkinson, *J. Phys. Chem. A* **2002**, *106*, 6121–6128.

[14] J. Jover, R. Bosque, J. Sales, *Dalton Trans.* **2008**, 6441–6453.

[15] J. Jover, R. Bosque, J. Sales, *J. Phys. Chem. A* **2009**, *113*, 3703–3708.

[16] V. W.-M. Lee, H. Li, T.-C. Lau, R. Guevremont, K. W. M. Siu, *J. Am. Soc. Mass Spectrom.* **1998**, *9*, 760–766.

[17] a) C. B. Acland, H. C. Freeman, *J. Chem. Soc. D* **1971**, 1016–1017; b) M. E. Kamwaya, E. Papapvinsam, S. G. Teoh, R. K. Rajaram, *Acta Crystallogr. Sect. A Acta Crystallogr. C* **1984**, *40*, 1318–1320; c) A. Démaret, F. Abraham, *Acta Crystallogr. Sect. A Acta Crystallogr. C* **1987**, *43*, 1519–1521; d) K. Nomiya, S. Takahashi, R. Noguchi, S. Nemoto, T. Takayama, M. Oda, *Inorg. Chem.* **2000**, *39*, 3301–3311; e) K. Nomiya, H. Yokoyama, *J. Chem. Soc. Dalton Trans.* **2002**, 2483–2490; f) L. Wang, Y. Pei, *Acta Crystallogr. Sect. A Acta Crystallogr. E.* **2006**, *62*, m1487–m1488; g) N. C. Kasuga, M. Sato, A. Amano, A. Hara, S. Tsuruta, A. Sugie, K. Nomiya, *Inorg. Chim. Acta* **2008**, *361*, 1267–1273; h) N. C. Kasuga, Y. Takagi, S. Tsuruta, W. Kuwana, R. Yoshikawa, K. Nomiya, *Inorg. Chim. Acta* **2011**, *368*, 44–48; i) N. C. Kasuga, R. Yoshikawa, Y. Sakai, K. Nomiya, *Inorg. Chem.* **2012**, *51*, 1640–1647.

[18] a) T. Jayasekharan, N. K. Sahoo, *Rapid Commun. Mass Spectrom.* **2010**, *24*, 3562–3566; b) I. K. Chu, D. M. Cox, X. Guo, I. Kireeva, T.-C. Lau, J. C. McDermott, K. W. M. Siu, *Anal. Chem.* **2002**, *74*, 2072–2082.

[19] a) J.-S. Shen, D.-H. Li, M.-B. Zhang, J. Zhou, H. Zhang, Y.-B. Jiang, *Langmuir* **2011**, *27*, 481–486; b) J. Nan, X.-P. Yan, *Chem. Eur. J.* **2010**, *16*, 423–427.

[20] R. M. C. Dawson, D. C. Elliott, W. H. Elliott, *Data for Biochemical Research*, Clarendon Press, Oxford, **1959**.

[21] A. F. Holleman, N. Wiberg, *Lehrbuch der Anorganischen Chemie*, 102 ed., Walther de Gruyter, Berlin, **2007**.

[22] For example, see: a) T. Köchner, N. Trapp, T. A. Engesser, A. J. Lehner, C. Röhr, S. Riedel, C. Knapp, H. Scherer, I. Krossing, *Angew. Chem.* **2011**, *123*, 11449–11452; *Angew. Chem. Int. Ed.* **2011**, *50*, 11253–11256; b) M. Risto, T. T. Takaluoma, T. Bajorek, R. Oilunkaniemi, R. S. Laitinen, T. Chivers, *Inorg. Chem.* **2009**, *48*, 6271–6279.

[23] J. B. Stock, B. Rauch, S. Roseman, *J. Biol. Chem.* **1977**, *252*, 7850–7861.

[24] I. Bagai, C. Rensing, N. J. Blackburn, M. M. McEvoy, *Biochemistry* **2008**, *47*, 11408–11414.

[25] E.-H. Kim, D. H. Nies, M. M. McEvoy, C. Rensing, *J. Bacteriol.* **2011**, *193*, 2381–2387.

[26] G. R. Fulmer, A. J. M. Miller, N. H. Sherden, H. E. Gottlieb, A. Nudelman, B. M. Stoltz, J. E. Bervaw, K. I. Goldberg, *Organometallics* **2010**, *29*, 2176–2179.

[27] CCDC-840724 (**1**), CCDC-840725 (**2**), and CCDC-840726 (**3**) contain the supplementary crystallographic data for this paper. These data can be obtained free of charge from The Cambridge Crystallographic Data Centre via www.ccdc.cam.ac.uk/data_request/cif.

[28] E. Blanc, D. Schwarzenbach, H. D. Flack, *J. Appl. Crystallogr.* **1991**, *24*, 1035–1041.

[29] G. M. Sheldrick, SHELX-97, Program For Crystal Structure Refinement, University of Göttingen, Göttingen, **1997**.

[30] M. C. Burla, R. Caliandro, M. Camalli, B. Carrozzini, G. L. Cascarano, L. De Caro, C. Giacovazzo, G. Polidori, R. Spagna, *J. Appl. Crystallogr.* **2005**, *38*, 381–388.

[31] K. Brandenburger, DIAMOND Vers. 3.2 g, Visual crystal structure information system, Crystal Impact GbR, Bonn, **1997–2011**.

[32] Gaussian 09, Revision D.02, M. J. Frisch, G. W. Trucks, H. B. Schlegel, G. E. Scuseria, M. A. Robb, J. R. Cheeseman, G. Scalmani, V. Barone, B. Mennucci, G. A. Petersson, H. Nakatsuji, M. Caricato, X. Li, H. P. Hratchian, A. F. Izmaylov, J. Bloino, G. Zheng, J. L. Sonnenberg, M. Hada, M. Ehara, K. Toyota, R. Fukuda, J. Hasegawa, M. Ishida, T. Nakajima, Y. Honda, O. Kitao, H. Nakai, T. Vreven, J. A. Montgomery, Jr., J. E. Peralta, F. Ogliaro, M. Bearpark, J. J. Heyd, E. Brothers, K. N. Kudin, V. N. Staroverov, R. Kobayashi, J. Normand, K. Raghavachari, A. Rendell, J. C. Burant, S. S. Iyengar, J. Tomasi, M. Cossi, N. Rega, J. M. Millam, M. Klene, J. E. Knox, J. B. Cross, V. Bakken, C. Adamo, J. Jaramillo, R. Gomperts, R. E. Stratmann, O. Yazyev, A. J. Austin, R. Cammi, C. Pomelli, J. W. Ochterski, R. L. Martin, K. Morokuma, V. G. Zakrzewski, G. A. Voth, P. Salvador, J. J. Dannenberg, S. Dapprich, A. D. Daniels, Ö. Farkas, J. B. Foresman, J. V. Ortiz, J. Cioslowski, D. J. Fox, Gaussian, Inc., Wallingford CT, **2004**.

[33] A. Becke, *J. Chem. Phys.* **1993**, *98*, 5648–5652.

[34] W. R. Wadt, P. J. Hay, *J. Chem. Phys.* **1985**, *82*, 270–283.

[35] R. Ditchfield, W. J. Hehre, J. A. Pople, *J. Chem. Phys.* **1971**, *54*, 724–728.

[36] A. E. Reed, R. B. Weinstock, F. Weinhold, *J. Chem. Phys.* **1985**, *83*, 735–746.

R